

Ground-state search in multicomponent magnetic systems

Yu Kumagai,^{1,*} Atsuto Seko,¹ Fumiyasu Oba,¹ and Isao Tanaka^{1,2}

¹*Department of Materials Science and Engineering, Kyoto University, Kyoto 606-8501, Japan*

²*Nanostructures Research Laboratory, Japan Fine Ceramics Center, Nagoya 456-8587, Japan*

(Received 23 March 2011; revised manuscript received 3 October 2011; published 9 January 2012)

When the ground-state (GS) structures in multicomponent magnetic systems are explored using theoretical calculations, magnetic configurations must be considered as well as atomic configurations. However, an exhaustive search of the GS in both atomic and magnetic configurational spaces is prohibitively expensive. In this study, we present a cluster-expansion scheme to determine GS structures in multicomponent magnetic systems via a search in a reduced configurational space. The effectiveness of the scheme is illustrated by examining the GS structures in the MgO-NiO system, which is known as an exceptional rocksalt alloy that exhibits negative enthalpy of mixing.

DOI: [10.1103/PhysRevB.85.012401](https://doi.org/10.1103/PhysRevB.85.012401)

PACS number(s): 75.25.-j, 61.50.Ah, 61.66.Dk, 71.15.-m

I. INTRODUCTION

Multicomponent magnetic systems including transition-metal compounds exhibit a rich variety of fascinating characteristics and have technologically important applications such as spintronics [e.g., Mn-doped GaAs (Ref. 1)], lithium-ion batteries [e.g., Li_xCoO_2 (Refs. 2 and 3)], and thermoelectric devices [e.g., Na_xCoO_2 (Ref. 4)]. Since their physical properties depend on the atomic and magnetic configurations, it is essential to elucidate both atomic and magnetic configurations as a function of composition. When the ground-state (GS) structures in multicomponent magnetic systems are explored using theoretical calculations based on density functional theory (DFT), we have to consider the dependence of energetics not only on the atomic configurations, but also on magnetic configurations. However, it is prohibitively expensive to search in whole the configurational spaces in both degrees of freedom.

One of the solutions to overcome the difficulty is a combination of the cluster-expansion (CE) technique⁵⁻⁷ and DFT calculations. The CE generally considers only the atomic configurations. In ferromagnetic (FM) systems, the GS structures can be obtained by the conventional CE on the premise that the systems take FM configurations throughout the whole range of the atomic composition. In contrast, the magnetic configuration dependence must be considered for antiferromagnetic (AF) and ferrimagnetic systems. Alloys with weak AF or ferrimagnetic interactions have been treated by approximating the magnetic contribution using the FM configuration,⁸ but such an approximation fails when the magnetic interactions are sizable.⁹ An explicit treatment of the magnetic configuration together with the atomic configuration, however, results in a significant increase in computational cost.

In this paper, we present a procedure based on the CE to identify the GS structures in the multicomponent magnetic systems. This procedure enables us to search for the GS structures in the whole range of both the atomic and magnetic configurational spaces. Although we here focus on multicomponent magnetic systems, it is in principle applicable to a wide range of systems with any two or more configurational degrees of freedom by using an analogy with the relationship between the atomic and magnetic degrees of freedom in the multicomponent magnetic systems. For instance, in the case of multicomponent systems with multivalent atoms, the magnetic configuration is replaced by the charge configuration.

The procedure is illustrated by applying it to the MgO-NiO alloy, in which magnetic interactions play an important role to determine the GS structures as shown later. Experimentally, MgO-NiO solid solutions with the rocksalt structure are known to form around 1400 K (Refs. 10–13) throughout the whole composition range. Among many combinations of binary oxides, the MgO-NiO alloy is known as an exceptional rocksalt alloy that exhibits negative enthalpy of mixing, indicating a tendency toward ordering at low temperature.^{14,15} However, the GS structures have been unknown both experimentally and theoretically.

II. THEORETICAL DETAILS

A. Cluster-expansion method

In the CE, the configurational energy in a nonmagnetic binary system E is expanded as a function of the atomic configuration σ :

$$E(\sigma) = V_0 + \sum_i V_i \langle \sigma_i \rangle + \sum_{i,j} V_{i,j} \langle \sigma_i \sigma_j \rangle + \dots, \quad (1)$$

where the pseudospin variable σ_i represents the atomic species on lattice site i . $\langle \sigma_i \sigma_j \rangle$ are correlation functions. The number of pseudospin variables in the angle bracket corresponds to the cluster size. The expansion coefficients V are called effective cluster interactions (ECIs), which characterize the energetics of the system. Once the ECIs are estimated from the energies by DFT calculations, the configurational energy can be evaluated rapidly.

B. Energetics of multicomponent magnetic system

We consider the situation that the structure with the minimum energy is searched for in a multicomponent magnetic system with a constant composition. As schematically illustrated in Fig. 1(a), the total energy of the system is a function of atomic and magnetic configurations. When the magnetic moment of an atom on lattice site i is expressed as a continuous three-dimensional spin vector s_i , the structure with the minimum energy satisfies

$$E^{\min} = \min_{\sigma} [\min_s E(\sigma, s)], \quad (2)$$

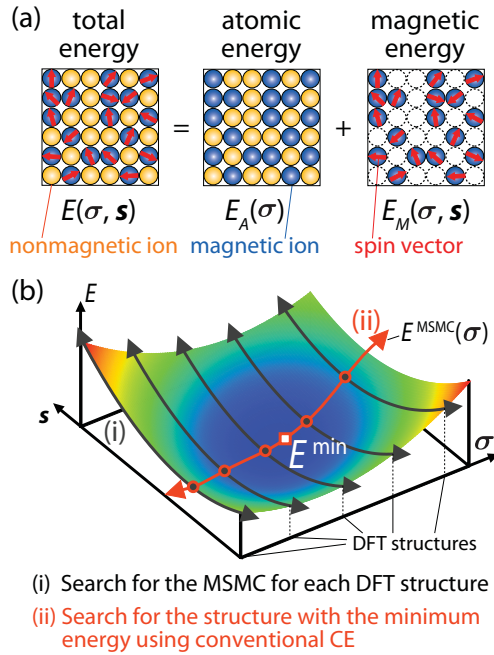


FIG. 1. (Color online) Schematic illustrations of (a) energetics and (b) configurational space used for the search for the minimum energy structure in multicomponent magnetic systems. The process for determining the structure with the minimum energy is divided into two main parts. The MSMC for each atomic configuration is first searched for. The structure with the minimum energy is then explored among the structures with the MSMCs.

where $E(\sigma, s)$ denotes the energy of a structure as a function of σ and the magnetic configuration $s = \{s_1, s_2, \dots, s_N\}$. When lattice site i is occupied with a nonmagnetic ion, the zero vector is substituted for s_i . Since an exhaustive search in both atomic and magnetic configurational spaces is computationally expensive, we propose an alternative scheme that can significantly reduce the configurational space used for the search by exploring the most stable magnetic configurations (MSMCs) only for input DFT structures.

The energy of a structure in a magnetic system can be divided into two parts. One is a contribution to the energy dependent on the magnetic configuration, defined as the magnetic interaction energy E_M . The other is the remaining part of the energy, which is independent of the magnetic configuration. This can be called the atomic interaction energy E_A . Then, the energy is expressed as

$$E(\sigma, s) = E_A(\sigma) + E_M(\sigma, s). \quad (3)$$

E_M is generally a function of both atomic and magnetic configurations. When using the classical Heisenberg model for the magnetic interaction energy, E_M is described as

$$E_M(\sigma, s) = \sum_{i,j} J_{i,j}(\sigma) s_i \cdot s_j, \quad (4)$$

where $J_{i,j}$ are magnetic pair interactions. E_A corresponds to the energy of a structure with a completely random magnetic configuration, where correlations between spin pairs vanish, and depends only on the atomic configuration.

By combining Eq. (2) with Eq. (3), the minimum energy is rewritten using the energy of a structure with the MSMC, E^{MSMC} , as

$$\begin{aligned} E^{\text{min}} &= \min_{\sigma} [E_A(\sigma) + \min_s [E_M(\sigma, s)]] \\ &= \min_{\sigma} [E^{\text{MSMC}}(\sigma)]. \end{aligned} \quad (5)$$

This equation implies that the structure with the minimum energy can be explored only in the atomic configurational space using the CE once the MSMCs for input atomic configurations are determined and their DFT energies are estimated. The situation is schematically illustrated in Fig. 1(b). We can expand the energies as

$$\begin{aligned} E^{\text{MSMC}}(\sigma) &= V_0^{\text{MSMC}} + \sum_i V_i^{\text{MSMC}}(\sigma_i) \\ &+ \sum_{i,j} V_{i,j}^{\text{MSMC}}(\sigma_i \sigma_j) + \dots, \end{aligned} \quad (6)$$

where V^{MSMC} denote ECIs for structures with the MSMCs. The ECIs contain the magnetic interactions of the MSMCs in addition to the atomic interactions.

C. Procedure for finding GS structures in multicomponent magnetic system

The practical procedure for determining the GS structures is shown in Fig. 2. We first determine the MSMCs for the input atomic configurations as follows: (i) Calculate DFT energies for structures with various atomic and magnetic configurations (steps 1–3). (ii) Estimate magnetic interactions J (step 4). In this study, the atomic and magnetic interaction energies are described by the usual CE formalism in Eq. (1) and the Heisenberg model in Eq. (4), respectively. The ECIs and magnetic interactions are simultaneously determined from DFT energies obtained at step 3. Although $J_{i,j}$ are generally dependent on the atomic configuration σ , we assumed $J_{i,j}$ to be independent of the atomic configuration in the MgO-NiO

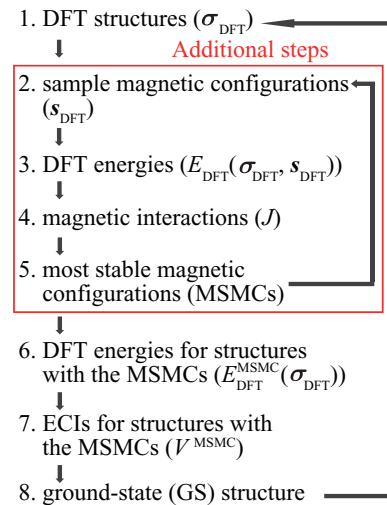


FIG. 2. (Color online) Flowchart of our CE procedure for determining the GS structures in magnetic systems. Additional steps for determining the MSMCs are inserted into the conventional CE procedure.

system. This approximation is justified by the fact that the DFT energies are well reproduced as shown later. (iii) Search for the MSMC for each input atomic configuration using the obtained magnetic interactions $J_{i,j}$ via simulated annealing¹⁶ (SA) (step 5). The MSMCs are iteratively determined by repeating steps 2–5 until no new MSMCs are predicted. After determining the MSMCs, the DFT energies of the structures with the MSMCs, $E_{\text{DFT}}^{\text{MSMC}}$, are calculated (step 6). Then, ECIs for structures with the MSMCs, V^{MSMC} , are obtained from $E_{\text{DFT}}^{\text{MSMC}}$ using Eq. (6) (step 7). Finally, the GS structures are identified using V^{MSMC} via the conventional CE procedure (step 8). The GS structures are also iteratively determined until no other GS structures are predicted through all steps.

In addition to the examination of the convergence of the GS structures, it is important to evaluate the accuracy of the ECIs and magnetic interactions. We adopted the leave-one-out cross-validation (CV) score to evaluate the predictive capability of the CE.^{17,18} In steps 4 and 7, the combination of the ECIs and the interaction range of the magnetic interactions are optimized by minimizing the CV score. However, the minimized CV score is not necessarily robust for estimating the accuracy of the ECIs and magnetic interactions since the leave-one-out CV score is a statistical quantity. Therefore, convergence of the CV score with respect to the number of DFT structures is carefully examined.¹⁹

III. COMPUTATIONAL DETAILS

For the DFT calculations, 76 input atomic configurations were used in a 64-atom supercell constructed by the $2 \times 2 \times 2$ expansion of the conventional rocksalt unit cell. The input atomic configurations were distributed at intervals of 6.25% composition, including pure MgO and NiO. Since the sublattice of oxygen atoms is common to all compositions, the oxygen atoms are not considered in the CE. For each atomic configuration, a set of magnetic configurations was also prepared. To reduce the computational cost of DFT calculations, we only considered collinear magnetic configurations. The initial set of magnetic configurations S_{DFT} was randomly selected.

Spin-polarized DFT calculations were performed using projector-augmented-wave (PAW) method²⁰ and the Perdew-Burke-Ernzerhof generalized gradient approximation²¹ (GGA) as implemented in the VASP code.^{22,23} Mg $3s$, Ni $3d$ and $4s$, and O $2s$ and $2p$ electrons were treated as valence electrons. The PAW radial cutoffs for Mg, Ni, and O were 1.1, 1.2, and 0.8 Å, respectively. A Γ -centered $3 \times 3 \times 3$ k -point mesh was used for the Brillouin-zone integration of the supercells. Geometry optimization was performed until the Hellmann-Feynman force acting on each atom was reduced to less than 0.01 eV/Å. Wave functions were expanded with plane waves up to 600 eV. We treated strong onsite Coulomb interactions on the localized Ni $3d$ orbitals with the GGA + U using the simplified rotationally invariant approach.²⁴ An effective U value of 5 eV, which reproduces the experimental first-nearest-neighbor (1st NN) and second-nearest-neighbor (2nd NN) magnetic interactions of rocksalt NiO, was adopted. The 1st NN and 2nd NN magnetic interactions of NiO were estimated from the energies for FM, type-I AF, and type-II AF configurations

based on the classical Heisenberg model Hamiltonian $H = \sum_{1\text{st NN}} J_1 s_i \cdot s_j + \sum_{2\text{nd NN}} J_2 s_i \cdot s_j$ ($|s| = 1$ for NiO). The calculated 1st NN and 2nd NN magnetic interactions of -1.39 and 17.54 meV, respectively, are close to previously reported experimental values of -1.37 and 19.01 meV.²⁵

IV. RESULTS AND DISCUSSION

Using the DFT energies, atomic ECIs and magnetic pair interactions were obtained. We used the leave-one-out CV score to evaluate the predictive capability of the CE. Minimization of the CV score, where short-distance pair interactions were included without selection, was performed by selecting clusters using the genetic algorithm.²⁶ The many-body clusters considered in the selection were 23 triplets and 3 quadruplets in which cation-cation distances are less than or equal to the distances of the 6th and 2nd NN pairs, respectively. The ECIs for the selected clusters were estimated by a least-squares-fitting procedure. We used the CLUPAN code^{19,27} in the series of CE calculations. The minimized CV score, which converges with respect to the number of input DFT structures, is 0.75 meV/cation. In the present approach, the error of the CE partly originates from the approximation that the magnetic interactions are independent of the atomic configuration. However, the small value of the CV score indicates that spin-polarized DFT energies are well reproduced using the approximation.

Figure 3(a) shows the calculated atomic ECIs and magnetic pair interactions. We found that the contributions of the many-body clusters to the total energies are relatively small. Among the atomic interactions, only pair ECIs have a dominant role in predicting the GS. The atomic pair ECI decreases monotonically and approaches zero with increasing distance. The 1st NN atomic ECI is large and positive, which implies a strong ordering tendency of forming the 1st NN Mg-Ni pairs. Among the Ni-Ni magnetic interactions, the 2nd NN AF interaction is the strongest, which is attributed to the

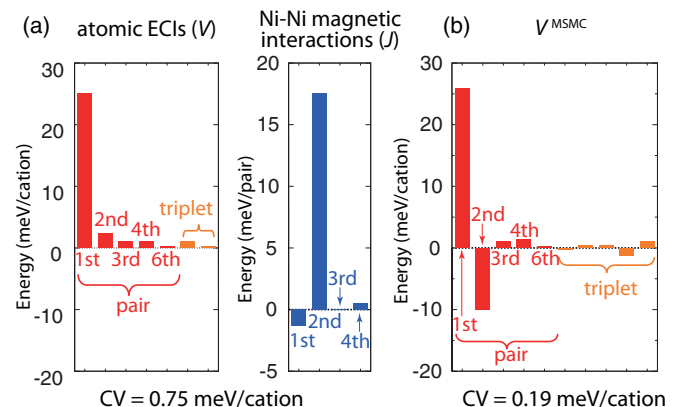


FIG. 3. (Color online) (a) Atomic ECIs and Ni-Ni magnetic interactions in the MgO-NiO system. (b) ECIs applicable for structures with the MSMCs. The pseudospin variables $\sigma_i = +1$ and -1 correspond to the Mg and Ni atoms, respectively. The 5th NN pair interaction is not considered for atomic interactions since the correlation function of the 5th NN pair is equivalent to that of the 1st NN pair in the periodic $2 \times 2 \times 2$ supercell. CV denotes the leave-one-out cross-validation score.

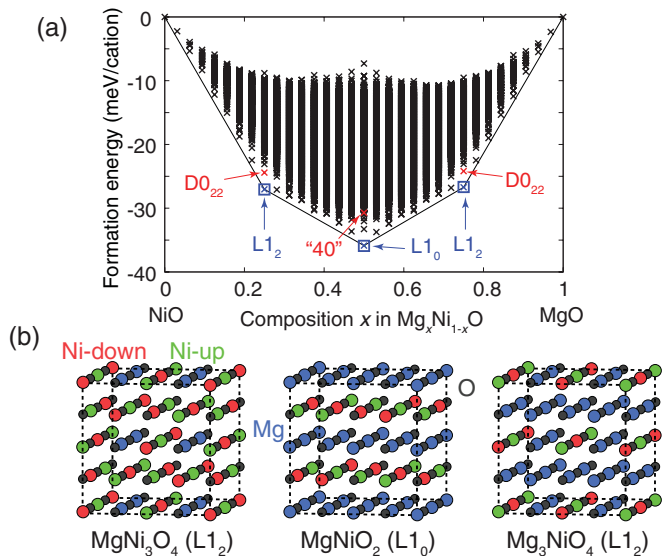


FIG. 4. (Color online) (a) Formation energies for all atomic configurations in the $2 \times 2 \times 2$ supercell and (b) identified GS structures. The formation energy of a structure with composition x is defined as $E_f(x) = E_{\text{Mg}_x\text{Ni}_{1-x}\text{O}} - [xE_{\text{MgO}} + (1-x)E_{\text{NiO}}]$. The squares show the DFT formation energies of the GS structures. In the GS structures, the 2nd and 4th NN Ni-Ni pairs possess fully AF and FM configurations, respectively, whereas the 1st and 3rd NN pairs hold both FM and AF configurations equally. DO_{22} and “40,” which are A_1B_3 and A_2B_2 superlattices along the $[012]$ direction (Ref. 28), respectively, are the structures predicted by considering only atomic interactions.

superexchange interactions mediated by oxygen ions. Through the steps 6 and 7, the calculated V^{MSMC} values are also shown in Fig. 3(b). Reflecting the strong AF interaction of the 2nd NN pairs, the 2nd NN V^{MSMC} is opposite in sign to the 2nd NN atomic ECI.

Using V^{MSMC} , we identified the GS structures. We first calculated the energies for all atomic configurations within the $2 \times 2 \times 2$ supercell (32 cations). The number of configurations is about 2×10^9 . Figure 4 shows the formation energies for all configurations. The formation energy of the GS structure is lower than not only any other structures at its composition, but also the linear combination of energies of any two structures at the same composition. In Fig. 4(a), we found three GS structures at $x = 0.25, 0.5,$ and 0.75 , which have L_{1_2} -, L_{1_0} -, and L_{1_2} -type atomic configurations, respectively. These structures are also confirmed using SA performed with $3 \times 3 \times 3, 4 \times 4 \times 4,$ and $5 \times 5 \times 5$ supercells. In the L_{1_0} and L_{1_2} structures, the 1st and 2nd NN pairs are maximally formed by different and the same types of cations, respectively. The MSMCs for the GS structures were also determined using SA. The identified atomic and magnetic configurations of the GS structures are shown in Fig. 4(b).

To clarify the origin of the negative formation energies of the GS structures, we divide the formation energies into the atomic and magnetic contributions. The atomic contributions are estimated from the atomic ECIs. The magnetic contributions for the structures with the MSMCs, E_M^{MSMC} , are evaluated from the residual between the formation energies and the atomic contributions as $E_M^{\text{MSMC}}(\sigma) = E^{\text{MSMC}}(\sigma) - E_A(\sigma)$. The atomic and magnetic contributions for all configurations

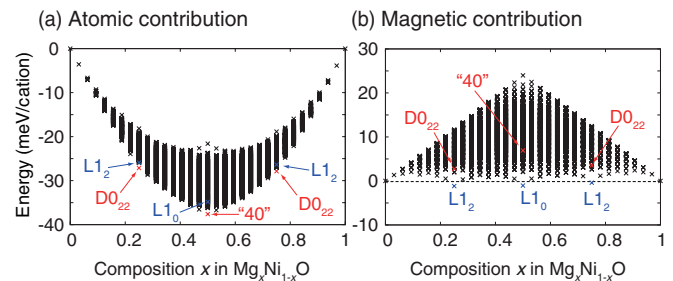


FIG. 5. (Color online) Contributions of (a) atomic and (b) magnetic interactions to the formation energies.

within the $2 \times 2 \times 2$ supercell are shown in Figs. 5(a) and 5(b), respectively. The atomic contributions are negative in all the configurations. When only the atomic contributions are considered, the DO_{22} , “40,” and DO_{22} structures are most stable at $x = 0.25, 0.5,$ and 0.75 , respectively.

In contrast to the atomic contributions, the magnetic contributions are positive in almost all configurations. This finding can be mostly explained by the number of 2nd NN Ni-Ni pairs that dominate the magnetic interactions as shown in Fig. 3(a). When the number of 2nd NN Ni-Ni pairs in a structure is less than that in the phase-separated state, in which the system segregates to the pure MgO and NiO, the magnetic contribution is positive. Since the “40” structure contains two 2nd NN Ni-Ni pairs per Ni ion, corresponding to two-thirds of the number of 2nd NN Ni-Ni pairs in the phase-separated state, the magnetic contribution is positive. On the other hand, the L_{1_0} structure contains the same number of 2nd NN Ni-Ni pairs as the phase-separated state, and the magnetic contribution is close to zero. Strictly speaking, the magnetic contributions should be exactly zero since the numbers of magnetic interactions up to the 4th NN in L_{1_0} and L_{1_2} are the same as those in the phase-separated states. The deviations from zero of less than 1.2 meV/cation found in Fig. 5(b) are caused by the CE fitting errors. This analysis indicates that the magnetic interaction destabilizes the cation-ordering tendencies in most structures. As a result, the L_{1_0} structure is relatively well stabilized as shown in Fig. 4(a). The same holds for the stabilization of the L_{1_2} structure at $x = 0.25$ and 0.75 .

V. SUMMARY

We propose a scheme for predicting the GS structures of multicomponent systems involving atoms with localized magnetic moments. It enables us to greatly reduce the configurational space used for the GS search. Using the proposed scheme, the GS structures of the MgO-NiO system, which have not been experimentally reported, are identified. The GS structures have the maximum number of geometrically permitted 2nd NN AF Ni-Ni pairs. The GS structures are relatively well stabilized by the magnetic interactions compared with other ordered structures, while their negative formation energies originate only from the atomic interactions.

ACKNOWLEDGEMENT

This work was supported by Grants-in-Aid for Young Scientists (A) and Priority Areas (No. 474) from MEXT of Japan.

*yuukuma@gmail.com

- ¹T. Dietl, *Nat. Mater.* **9**, 965 (2010).
- ²T. Motohashi, T. Ono, Y. Sugimoto, Y. Masubuchi, S. Kikkawa, R. Kanno, M. Karppinen, and H. Yamauchi, *Phys. Rev. B* **80**, 165114 (2009).
- ³K. Miyoshi, C. Iwai, H. Kondo, M. Miura, S. Nishigori, and J. Takeuchi, *Phys. Rev. B* **82**, 075113 (2010).
- ⁴R. Berthelot, D. Carlier, and C. Delmas, *Nat. Mater.* **10**, 74 (2011).
- ⁵J. M. Sanchez, F. Ducastelle, and D. Gratias, *Phys. A (Amsterdam)* **128**, 334 (1984).
- ⁶D. de Fontaine, *Solid State Physics* (Academic, New York, 1994), Vol. 47.
- ⁷F. Ducastelle, *Order and Phase Stability in Alloys* (Elsevier, New York, 1994).
- ⁸F. Zhou, T. Maxisch, and G. Ceder, *Phys. Rev. Lett.* **97**, 155704 (2006).
- ⁹M. Y. Lavrentiev, S. L. Dudarev, and D. Nguyen-Manh, *J. Nucl. Mater.* **22**, 386 (2009).
- ¹⁰E. Cazzanelli, A. Kuzmin, N. Mironova-Ulmane, and G. Mariotto, *Phys. Rev. B* **71**, 134415 (2005).
- ¹¹Z. Feng and M. S. Seehra, *Phys. Rev. B* **45**, 2184 (1992).
- ¹²K. V. Rao and C. S. Sunandana, *J. Phys. Chem. Solids* **69**, 87 (2008).
- ¹³A. Kuzmin and N. Mironova, *J. Phys.: Condens. Matter* **10**, 7937 (1998).
- ¹⁴P. K. Davies and A. Navrotsky, *J. Solid State Chem.* **38**, 264 (1981).
- ¹⁵P. K. Davies and A. Navrotsky, *J. Solid State Chem.* **46**, 1 (1983).
- ¹⁶J. S. Kirkpatrick, C. D. Gelatt, and M. P. Vecchi, *Science* **220**, 671 (1983).
- ¹⁷M. Stone, *J. R. Stat. Soc. B* **36**, 111 (1974).
- ¹⁸A. van de Walle and G. Ceder, *J. Phase Equilib.* **23**, 348 (2002).
- ¹⁹A. Seko, Y. Koyama, and I. Tanaka, *Phys. Rev. B* **80**, 165122 (2009).
- ²⁰P. E. Blöchl, *Phys. Rev. B* **50**, 17953 (1994).
- ²¹J. P. Perdew, K. Burke, and M. Ernzerhof, *Phys. Rev. Lett.* **77**, 3865 (1996).
- ²²G. Kresse and D. Joubert, *Phys. Rev. B* **59**, 1758 (1999).
- ²³G. Kresse and J. Furthmüller, *Phys. Rev. B* **54**, 11169 (1996).
- ²⁴S. L. Dudarev, G. A. Botton, S. Y. Savrasov, C. J. Humphreys, and A. P. Sutton, *Phys. Rev. B* **57**, 1505 (1998).
- ²⁵M. T. Hutchings and E. J. Samuelsen, *Phys. Rev. B* **6**, 3447 (1972).
- ²⁶G. L. W. Hart, V. Blum, M. J. Walorski, and A. Zunger, *Nat. Mater.* **4**, 391 (2005).
- ²⁷A. Seko [<http://sourceforge.net/projects/clupan>].
- ²⁸G. Sauthoff, *Intermetallics* (Wiley-VCH, Weinheim, 1995).